Towards a mathematical model for single molecule structured illumination microscopy

Mathias Hockmann[1,2]**, Stefan Kunis**[1,2*]**, and Rainer Kurre**[2]

[1] Osnabrueck University, Institute of Mathematics, Albrechtstr. 28a, 49076 Osnabrück

[2] Osnabrueck University, Research Center of Cellular Nanoanalytics, Barbarastr. 11, 49076 Osnabrück

Abstract: While structured illumination microscopy (SIM) is a widely used super-resolution microscopy technique for densely labelled samples, we apply a modified version of the matrix pencil method to single molecule imaging. We prove that under reasonable conditions we can recover up to two times more molecule positions compared to conventional microscopy exactly from noiseless data and include numerical examples illustrating benefits as well as limitations of the algorithm.

1 Introduction

Classical fluorescence microscopy used in many biological and medical applications suffers from the appearance of a limit for resolution caused by the diffraction of light. Broadly speaking, fluorescence microscopy means that a specimen labelled with a fluorescent marker is illuminated and the resulting fluorescence is observed through an optical system. From a mathematical point of view, the two-dimensional image data f measured by the microscope's digital detector are related to the distribution μ of the fluorescent markers by the convolution

$$f(x) = [(g \cdot \mu) * h](x), \quad x \in [0, 1]^2, \tag{1}$$

where $h : \mathbb{R}^2 \to \mathbb{R}$ is the *point spread function (PSF)* of the optical system and $g : \mathbb{R}^2 \to \mathbb{R}$ is the illumination pattern (cf. [6, 8]). Naturally, the task is then to deconvolve the data under the assumption that we know h and g. In conventional fluorescence microscopy, the illumination g is constant in the field of view and therefore we obtain $g \cdot \hat{\mu}(k) \cdot \hat{h}(k)$ by applying the Fourier transform on both sides of (1). This just allows to recover $\hat{\mu}$ on a disk around the origin because this is typically the support of $\hat{h}$.[1] Instead, one can also think about a more complicated illumination pattern g and this idea leads to *(linear) structured illumination microscopy* (SIM) (cf. [4, 6, 8]). Using the correspondence between modulation in real space and translation in frequency space, the image f contains not only the centered spectral information $\hat{\mu}$ but also shifted frequency data $\hat{\mu}(\cdot \pm k_0)$ if a sinusoidal illumination pattern with wave vector k_0 is generated. By measuring f for different choices of sinusoidal patterns g, one can separate the spectral components. Repeating the process with a rotated pattern allows to gain shifted spectral components in additional directions.
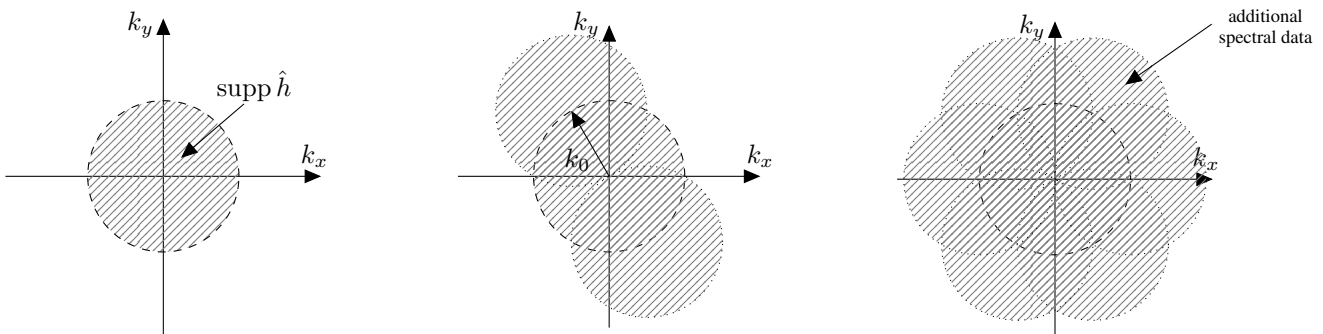

Fig. 1: 2D-SIM in frequency space: Conventional microscopy just allows to reconstruct the spectrum $\hat{\mu}$ on $\operatorname{supp} \hat{h}$ (left), SIM-images contain shifted spectral data in directions $\pm k_0$ (middle). By rotation of the pattern one obtains additional data in various directions (right).

To sum up, SIM provides spectral information about a function μ on a collection of shifted disks. For densely labelled samples the *Gustafsson method* is the processing routine which is widely used in applications of SIM (cf. [4, 8, 9]). However, this algorithm cannot be used in the case of single molecule imaging techniques where only a small number of single fluorescent emitters are present at the same time since the Gustafsson method tacitly assumes that $\hat{\mu}$ has few oscillations. But this is not

---

[*] Corresponding author: e-mail skunis@uos.de
[1] The radius of the circle depends on the diffraction limit by Ernst Abbe.

the case if μ is a linear combination of spikes located at the positions of the individual molecules. Instead, we introduce 2D SIM for sparsely labelled samples in section 2 and present our own approach for the univariate case in section 3 by adapting the *multivariate matrix pencil method* (cf. [1]). Additionally, we discuss possible extension to dimension two. Finally, we analyse whether the univariate method allows to reconstruct more molecules than conventional microscopy data in section 4.

2 2D structured illumination microscopy for sparsely labelled samples

In single molecule microscopy, we are interested in the reconstruction of the positions $x_j \in [0,1)^2$ and weights $\lambda_j > 0$, $j = 1, \ldots, R$, in the a-prior signal model

$$\mu(x) = \sum_{j=1}^{R} \lambda_j \delta(x - x_j), \tag{2}$$

from equidistant samples of its low-pass filtered version $(g \cdot \mu) * h$. After twodimensional discrete Fourier transforms and separation of spectral components, linear SIM acquires the frequency data

$$\hat{\mu}(k - mk_l) = \sum_{j=1}^{R} \lambda_j e^{-2\pi i \langle k - mk_l, x_j \rangle}, \quad m = -1, 0, 1, \quad l = 0, \ldots, L-1, \quad k \in \mathrm{supp}(\hat{h}) \cap \mathbb{Z}^2. \tag{3}$$

If the direction vectors have integer entries $k_l \in \mathbb{Z}^2$, the data is a classically sampled exponential sum and e.g. the techniques in [1] can be applied directly. Otherwise we lift the problem to an exponential sum in higher dimension via

$$= \sum_{j=1}^{R} \lambda_j e^{-2\pi i \langle k - mk_l, x_j \rangle} = \sum_{j=1}^{R} \lambda_j e^{-2\pi i \left\langle \binom{k}{m}, \binom{x_j}{\langle -k_l, x_j \rangle} \right\rangle} = \sum_{j=1}^{R} \lambda_j e^{-2\pi i \langle \tilde{k}, \tilde{x}_j \rangle}$$

with some more complicated frequencies $\tilde{k} = (k, m)^\top \in (\mathrm{supp}(\hat{h}) \cap \mathbb{Z}^2) \times \{m \in \mathbb{Z}^L : \|m\| \le 1\} \subset \mathbb{Z}^{2+L}$ and note that we are only interested in reconstructing the first two coordinates of the augmented nodes $\tilde{x}_j \in [0,1)^{2+L}$. Subsequently, we restrict our analysis to the case of only one direction, i.e., $L = 1$, and thus can also restrict ourselves to the one-dimensional setting.

3 Reconstruction algorithm for one direction and its recovery guarantee

In order to keep the notation simple we proceed by analysing the situation in the univariate case with one illumination direction. We define

$$\mathcal{T} = \begin{pmatrix} \hat{\mu}(k-l)_{0 \le k,l \le n} & \hat{\mu}(k-l-k_0)_{0 \le k,l \le n} \\ \hat{\mu}(k-l+k_0)_{0 \le k,l \le n} & \hat{\mu}(k-l)_{0 \le k,l \le n} \end{pmatrix} \in \mathbb{C}^{(2n+2) \times (2n+2)}. \tag{4}$$

and note that this matrix is a Toeplitz matrix for $k_0 = n + 1$ and a 2×2 block-Toeplitz matrix with Toeplitz blocks for $k_0 \in \mathbb{R}$. In general, we expect that its rank $r := \mathrm{rank}(\mathcal{T})$ can be larger than the rank of its upper left block containing the non-SIM data and this might allow for the recovery of more points. Direct computation shows the (non accessible) factorisation $\mathcal{T} = \mathcal{A}^* D \mathcal{A}$ with the generalised Vandermonde matrix

$$\mathcal{A} = \begin{pmatrix} \vdots & & \vdots & \vdots & & \vdots \\ z_j^0 & \cdots & z_j^n & z_j^{k_0} z_j^0 & \cdots & z_j^{k_0} z_j^n \\ \vdots & & \vdots & \vdots & & \vdots \end{pmatrix} \in \mathbb{C}^{R \times (2n+2)}$$

and the diagonal weight matrix $D = \mathrm{diag}(\lambda_1, \ldots, \lambda_R) \in \mathbb{R}^{R \times R}$, respectively. Instead, we compute the singular value decomposition $\mathcal{T} = U \Sigma V^*$ and define the matrices

$$S_1 = U^* \mathcal{T}_1 V \Sigma^{-1} \in \mathbb{C}^{r \times r}, \qquad \mathcal{T}_1 = \begin{pmatrix} \hat{\mu}(k-l+1)_{0 \le k,l \le n} & \hat{\mu}(k-l-k_0+1)_{0 \le k,l \le n} \\ \hat{\mu}(k-l+k_0+1)_{0 \le k,l \le n} & \hat{\mu}(k-l+1)_{0 \le k,l \le n} \end{pmatrix}.$$

Analogously to [1, Thm. 2.1], we can prove the following proposition about recovery of the nodes from SIM data.

Proposition 3.1 *If* $\mathrm{rank}\,\mathcal{A} = R$, *we can recover the points* $z_j = e^{-2\pi i x_j}$, $j = 1, \ldots, R$, *as eigenvalues of* S_1. *In other words, there is a regular matrix* $W \in \mathbb{C}^{R \times R}$ *and a permutation* τ *on* $1, \ldots, R$ *such that*

$$W^{-1} S_1 W = \mathrm{diag}(z_{\tau(1)}, \ldots, z_{\tau(R)}).$$

P r o o f. The condition on the rank of $\mathcal{A}$ implies that $\mathcal{T} = \mathcal{A}^* D \mathcal{A}$ has rank R and thus $S_1 \in \mathbb{C}^{R \times R}$ which is necessary to recover the R nodes by diagonalisation. Similar to the proof in [1, Thm. 2.1], we can check that $W_0 := (\mathcal{A}U)^* \in \mathbb{C}^{R \times R}$ is regular. Moreover, we have $\mathcal{T}_1 = \mathcal{A}^* D D_1 \mathcal{A}$ with $D_1 = \mathrm{diag}(z_1, \ldots, z_R)$ and thus

$$W_0^{-1} S_1 W_0 = (\mathcal{A}U)^{-*} U^* \mathcal{T}_1 V \Sigma^{-1} (\mathcal{A}U)^* = (\mathcal{A}U)^{-*} U^* \mathcal{T}_1 V \left(U^* \mathcal{A}^* D \mathcal{A} V \right)^{-1} (\mathcal{A}U)^* = D_1.$$

So S_1 has distinct eigenvalues $z_1, \ldots, z_R$ and any matrix W which diagonalises S_1 causes just a permutation of these eigenvalues.[2]   □

Proposition 3.1 directly leads to the following algorithm to reconstruct the nodes using SIM data.

Algorithm 1 Single molecule Pencil-SIM in 1D

Input: R and trig.moments $\hat{\mu}(k)$, $k \in \{-n-k_0, \ldots, n+1-k_0\} \cup \{-n, \ldots, n+1\} \cup \{-n+k_0, \ldots, n+1+k_0\}$

1. Compute the singular value decomposition of $\mathcal{T}$.

2. Construct and diagonalise the matrix S_1 in order to obtain the nodes x_j from $z_j = e^{-2\pi i x_j}$.

3. Solve the least squares problem $\|\mathcal{A}^* \lambda - \hat{\mu}\|$ for the weights λ_j.

Output: Nodes x_j and weights λ_j

Example 3.2 We apply this to $R = 6$ random nodes in the intervall $[0, 1]$ and sample exact SIM data for $n = 2$. Whereas the matrix pencil method [1] just allows to reconstruct $n + 1 = 3$ spikes, we can reconstruct all spikes up to machine precision by algorithm 1 (cf. figure 2).

Remark 3.3 Following [1], a generalisation to the two- and three-dimensional case for one illumination direction is achieved by setting up one shifted multilevel Toeplitz matrix $\mathcal{T}_j$ for each spatial dimension and realising the coordinates of the nodes as generalised eigenvalues of several pencils. Our approach extends to nonlinear SIM (cf. [5, 7, 8]) by considering more spectral components in (3) which results in more blocks of the matrix (4).

Finally, a generalisation to more than one illumination direction augments more virtual dimensions but its implications for the matrix (4) are not yet fully understood. All of these technically involved generalisations are future work to be discussed elsewhere.

4 Resolution enhancement in 1D

A first step towards an analysis of our approach is obviously to find quantitative conditions which are necessary or sufficient for $\mathrm{rank}\,\mathcal{A} = R$ as this was the assumption in proposition 3.1. Thinking of R satisfying $n + 1 < R \le 2n + 2$, this would mean that we could recover ensembles of molecules that could not be reconstructed by using only the conventional spectral data $(\hat{\mu}(k))_{k=-n,\ldots,n}$. Moreover, the shift parameter k_0 is usually chosen as large as physically and experimentally possible. Therefore, we can think of $k_0 \approx n + 1$ and one certainly finds $\mathrm{rank}\,\mathcal{A} = R$ for $k_0 = n + 1$ and distinct nodes by the standard theory for Vandermonde matrices. Consequently, we are interested in an interval around $n + 1$ for which this also holds.

Proposition 4.1 Assume $n + 1 < R \le 2n + 2$ and

$$|n + 1 - k_0| < \frac{\sigma_R(A)}{\pi\sqrt{R(R-n-1)}}, \qquad A = \left(z_j^k\right)_{\substack{j=1,\ldots R \\ k=0,\ldots,R-1}} \in \mathbb{C}^{R \times R},$$

where A denotes the standard Vandermonde matrix and $\sigma_R(A)$ its smallest singular value. Then we have $\mathrm{rank}\,\mathcal{A} = R$.

P r o o f. We exploit the decomposition

$$\mathcal{A}_{:,1:R} = A + \begin{pmatrix} 0 & \ldots & 0 & z_1^{n+1}(z_1^{k_0-n-1}-1) & \ldots & z_1^{R-1}(z_1^{k_0-n-1}-1) \\ \vdots & & \vdots & \vdots & & \vdots \\ 0 & \ldots & 0 & z_R^{n+1}(z_R^{k_0-n-1}-1) & \ldots & z_R^{R-1}(z_R^{k_0-n-1}-1) \end{pmatrix}$$

and call the second matrix E. Since a square matrix $I + M$ is invertible if $\|M\| < 1$ in some norm, one deduces that $\mathcal{A}$ has full rank if $\|A^{-1}E\| < 1$ for any norm. Taking the 2-norm leads to an estimate

$$\|A^{-1}E\|_2^2 \le \sigma_R(A)^{-2} \|E\|_2^2 \le \sigma_R(A)^{-2} \|E\|_F^2 \le \sigma_R(A)^{-2} R \cdot (R-n-1)\pi^2 |n+1-k_0|^2,$$

where we used the inequality $|z_j^{k_0-n-1} - 1|^2 = |e^{2\pi i x_j (n+1-k_0)} - 1|^2 = 4\sin^2(\pi(n+1-k_0)x_j) \le 4\left(\pi(n+1-k_0)\frac{1}{2}\right)^2 = \pi^2 |n+1-k_0|^2$.   □

---

[2] Surely, we can not access W_0 because it already requires knowledge about the nodes z_j.

We note in passing, that the condition on k_0 can be weakened and simplified in certain situations either by trading a somewhat smaller constant for a larger minimal singular value of a *rectangular* Vandermonde matrix or by using the 1-norm and the explicit result [3] for the norm of the inverse of a Vandermonde matrix. Our second result shows that $\operatorname{rank} \mathcal{A} = R$ almost surely.

Proposition 4.2 *Let $n + 1 < R \leq 2n + 2$. If the nodes $(x_j)_{j=1}^R$ are distinct, then the set of $k_0 \in \mathbb{R}$ such that $\operatorname{rank} \mathcal{A} \neq R$ consists of isolated points. Similarly, for fixed $k_0 \in \mathbb{R} \setminus \{-n, \ldots, n\}$ the set $\{(x_1, \ldots, x_R) \in [0,1)^R : \operatorname{rank} \mathcal{A} \neq R\}$ is of Lebesgue measure zero.*

P r o o f. Direct computation shows that $\mathcal{A}\mathcal{A}^*$ is unitarily equivalent to the matrix $(2 \sin((n+1)\pi(x_j - x_\ell)) \cos(k_0 \pi(x_j - x_\ell)) / \sin(\pi(x_j - x_\ell)))_{j,\ell=1,\ldots,R}$. Real analyticity of its determinant, which does not vanish for $k_0 = n+1$, and [2, Proposition 5.4.8] show the first claim. Analogously, the determinant is non-vanishing and real analytic as a function of the nodes x_j. Consequently, the second statement follows from [10, Proposition 1]. □

Example 4.3 Let $p : \mathbb{T} \to \mathbb{R}$, $p(u) = (1 + \frac{i}{2})u^{-4} + (-1 - i)u^{-1} + (-1 + i)u^1 + (1 - \frac{i}{2})u^4$, then

$$
\begin{array}{c|cccc}
y & 0 & 3/24 & 7/24 & 8/24 \\
\hline
p(e^{2\pi iy}) & 0 & -2 - 2\sqrt{2} & 1 - \sqrt{2} + \sqrt{3}/2 & -\sqrt{3}/2
\end{array}
$$
and $\frac{d}{dy} p(e^{2\pi iy})_{|y=0} = 4\pi > 0$.

By the intermediate value theorem, the function $y \mapsto p(e^{2\pi iy})$ has at least four zeros $y_1 = 0 < y_2 < y_3 = 1/4 < y_4 < 1/3$. Multiplying p by $e^{-2\pi i4y} \neq 0$ and setting $x_j = 3y_j \in [0,1)$, $j = 1, 2, 3, 4$, we see that the Fourier submatrix

$$
\mathcal{A} = \left(e^{-2\pi i\ell y_j}\right)_{\substack{j \in \{1,2,3,4\} \\ \ell \in \{0,3,5,8\}}} = \left(e^{-2\pi ikx_j}\right)_{\substack{j \in \{1,2,3,4\} \\ k \in \{0,1,5/3,8/3\}}}
$$

is rank deficient.

Example 4.4 Fixing the nodes x_1, x_2 and x_4 from example 4.3 we compute the spectral condition number $\operatorname{cond}(\mathcal{A})$ for $k_0 \in [0.9, 2.1]$ and $x_3 \in [-0.1, 1.1]$ in MATLAB (cf. figure 3). The result reveals numerical singularity of $\mathcal{A}$ not only for $x_1 = 0, x_2 \approx 0.060$ and $x_4 \approx 0.930$ where nodes collide but also on a non-trivial curve whose precise description is unknown to us. Instead, we can only apply proposition 4.1 on some thin set (white) around the line $k_0 = 2$ (blue). The red line with $k_0 = \frac{5}{3}$ corresponds to example 4.3 where the non-trivial additional singularity is at $x_3 = 0.75$. As stated in proposition 4.2, we observe that only isolated values of k_0 lead to singularity of $\mathcal{A}$ if $x_3 \notin \{x_1, x_2, x_4\}$.
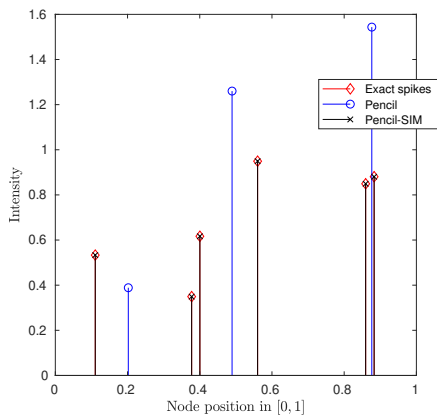

Fig. 2: Exact reconstruction of $R = 6$ spikes on $[0,1]$ using the Pencil-SIM method.
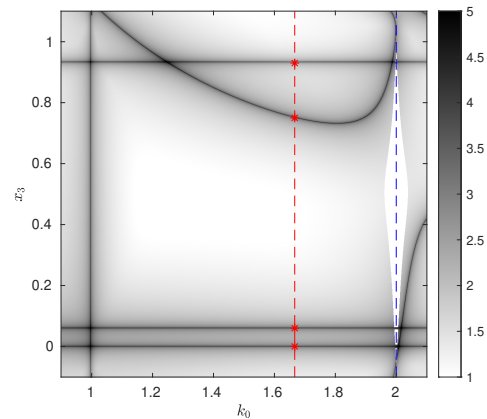

Fig. 3: Decimal logarithm of the condition number of $\mathcal{A}$ for varying spectral shift $k_0 \in [0.9, 2.1]$ and node $x_3 \in [-0.1, 1.1]$.

References

[1] M. Ehler, S. Kunis, T. Peter and C. Richter, Electron. Trans. Numer. Anal. **51**, 63-74 (2019).
[2] M. Field, Essential real analysis (Springer, Cham, 2017), pp. 182.
[3] W. Gautschi, Numer. Math. **4**, 117-123 (1962).
[4] M. G. L. Gustafsson, Journal of Microscopy **198**, 82-87 (2000).
[5] M. G. L. Gustafsson, PNAS **102**, 13081–13086 (2005).
[6] R. Heintzmann and C. Cremer, Proceedings SPIE 3568 (1999), pp. 185 – 196.
[7] R. Heintzmann, T. M. Jovin and C. Cremer, J. Opt. Soc. Am. A **19**, 1599–1609 (2002).
[8] E. A. Ingerman, R. A. London, R. Heintzmann and M. G. L. Gustafsson, Journal of Microscopy **273**, 3-25 (2019).
[9] A. Lal, C. Shan and P. Xi, IEEE Journal of Selected Topics in Quantum Electronics **22**, 50-63 (2016).
[10] B. S. Mityagin, Mathematical Notes **107**, 529-530 (2020).